Assessing Climate Vulnerability for Resilient Urban Planning:
A Multidiagnosis Approach

Eun Seok Lee[*]

Architecture and Urban Research Institute, KT and G Sejong Tower B 8F, 143, Gareum-ro, Sejong-si, 30116, Korea

Climate change and the inherent instability of cities create a significant threat to urban systems, and the impacts of climate change may worsen existing vulnerabilities in cities. In this study, we propose spatial solutions to enhance resilience in Korean cities facing climate change and minimize damages from natural disasters. To achieve this, we developed a vulnerability analysis model considering inadequate facilities and public-space utilization. We analyzed climate vulnerability under future scenarios, focusing on heat waves, urban flooding, and property damage in Korea, which are increasing in occurrence. By incorporating various climate-change-induced natural disaster factors into climate exposure variables, we identified current vulnerabilities within the context of future scenarios, allowing for the utilization of sensors and optimal monitoring locations for early preparedness. Future research could further establish criteria for designating natural disaster prevention districts and regulating development activities within such zones, as well as determining the best locations for heat wave and flood disaster prevention sensors.

1. Introduction

South Korea (36°N 128°E) is an East Asian country that experiences distinct seasonal changes and is exposed to a range of climate-change effects, such as drought, fine dust, heat waves, heavy rainfall, typhoons, cold waves, and heavy snowfall. In recent years, South Korea has experienced heat waves and heavy rainfall events that have resulted in significant loss of life and property damage. The year 2018 witnessed the longest heat wave period in South Korea's recorded history, spanning 31.5 days, which caused heat-related illnesses in 4457 individuals and led to 48 deaths.[1] In July 2011, Seoul, the capital city of South Korea, was severely affected by torrential rainfall that triggered landslides, leading to the loss of 57 lives, 12 missing individuals, and property damage worth $250 billion owing to damaged homes, flooded vehicles, and power outages.[2] Prior to 2010, South Korea had never experienced such extreme weather conditions.[3] Although such events have not yet directly caused large-scale loss of life and property, the risk escalates as the seasonal cycles of extreme weather events such as fine dust, drought, and cold waves intensify.[4,5]

Climate change and inherent urban insecurity are likely to combine and pose a significant threat to urban systems. Therefore, it is necessary to acknowledge that climate change can exacerbate urban insecurity.

To enhance the resilience of cities, it is essential to assess their current situation. This assessment should consider the combined threats of climate change and urban insecurity, and the results should be used for urban planning to build more resilient cities.[6,7] According to Sharifi and Yamagata,[8] urban resilience is important in dealing with climate change, and by considering the potential impacts of climate change and inherent urban insecurity, cities can be better prepared to withstand and recover from future environmental shocks and stresses.[9] In 1973, Holling defined resilience to be a tool for measuring a system's ability to absorb changes in its state variables and parameters while maintaining the status quo.[10] The word *resilience* is derived from the Latin word *resilio* meaning "to return to place".[11] Thus, urban resilience is defined as the ability of a system, community, or society to resist, absorb, or mitigate hazards promptly while keeping intact underlying structures and capacities. In the context of climate change, urban sustainability involves the maintenance of functions and controls by building resilience against potential vulnerabilities that can cause functional disruptions.[12] Meerow and Newell analyzed 172 articles on urban resilience published between 1973 and 2013 and defined urban resilience as the ability of urban systems and their corresponding socioecological and sociotechnical networks to maintain or return to a desirable level of functioning rapidly and adapt to change when exchanges occur across space and time.[13] The governance of cities, including factors such as polycentricity, transparency, accountability, flexibility, and inclusiveness, can influence the promotion of resilience. Improving the resilience of cities requires the convergence of social, policy, economic, and technological innovations.[14,15]

Several vulnerability assessment models have been developed to address specific natural hazards that cities may face. For instance, Meerow and Newell utilized urban statistical data to identify indicators of vulnerability in Detroit, USA, and utilized the results to map vulnerable areas in the city, thus enabling policymakers to enhance climate resilience.[13] Serre *et al.* developed a quantitative analysis tool, the DS3 model, to evaluate the flood resilience of neighborhoods in Hamburg, Germany.[16] They discovered that design factors such as transportation infrastructure, land use, and buildings significantly contributed to a neighborhood's flood resilience. To address an issue that urban designers frequently overlook, Feliciotti *et al.* proposed linking urban form elements to resilience.[17] Furthermore, extended models for diagnosing vulnerability have been introduced and classified into four types— hazard-disaster model, social vulnerability, integrated analysis, and extended vulnerability analysis—depending on whether they focus on physiobiological or socioeconomic factors as drivers of vulnerability.[18–20]

The objective of enhancing a city's ability to respond to disasters and minimize the scale of damage can be summarized as the goal of urban resilience.[21] The aim of this study is to propose spatial solutions for Korean cities exposed to climate change to minimize the scale of damage, enable rapid recovery, and improve resilience to natural disasters. To achieve this, a methodology was used to diagnose the vulnerability of the city to climate change and quantitatively determine its resilience. Geographic information analysis was employed to identify high-vulnerability

areas inside the city, which tend to be repeatedly exposed to natural disasters caused by climate change, and the vulnerability characteristics of buildings in such areas.[22] How the spatial elements of the analyzed cities were organized with respect to their sensitivity to damage and adaptive capacity to mitigate damage was also examined. The aim of this study is to provide a spatial basis for understanding the regional and geographical characteristics of areas currently vulnerable to climate-change-induced natural hazards in cities and to develop resiliency plans to minimize natural-hazard-linked damage. Additionally, through an analysis of location information for vulnerable areas in accordance with their specific characteristics, this study provides valuable insights into optimal sites for implementing disaster prevention technologies, including sensor-based prediction, monitoring, and warning systems for heat waves and floods.

2.   Materials and Methods

2.1   Indicators for vulnerability assessment

The vulnerability diagnostics in this study utilize the vulnerability analysis function of the Intergovernmental Panel on Climate Change (IPCC).[23] This function defines vulnerability as a positive relationship between exposure to climate impacts and a target's sensitivity and a negative relationship between a target's adaptive capacity [Eq. (1)].[23] Higher values of the vulnerability analysis function indicate higher vulnerability to climate change. This function can be applied differently depending on the natural disaster. In this study, we focused on heat waves and urban flooding as natural hazards caused by climate change. To limit the scope of this study, we used specific research definitions of exposure, sensitivity, and adaptive capacity for the climate-change vulnerability analysis. Exposure is based on indicators that can be used to predict future weather changes under representative concentration pathway (RCP) scenarios, such as heat waves and urban flooding. Sensitivity is based on quantitative indicators of urban buildings, infrastructure, and other components affected by climate change using publicly available spatial information. Adaptive capacity is based on indicators that describe the quantitative characteristics of urban components that can mitigate climate impact or overcome any damage.

$$(V) = f\left(I, S, A\right) = \sum_1^n E\left(x\right) + \sum_1^m S\left(y\right) - \sum_1^p A\left(z\right) \tag{1}$$

Here, V is vulnerability, I is exposure, S is sensitivity, and A is adaptive capacity.

As vulnerability diagnosis utilizes publicly available data from various organizations related to weather, administration, and architecture, there can be substantial variation in the values obtained. To minimize the error of outliers, Z-score standardization was applied to geocode the underlying data using Geographic Information System (GIS). The results were then organized using min–max normalization to a value between 0 and 1. Both Z-score standardization and min–max normalization were applied to the underlying data of climate exposure, sensitivity, and adaptive capacity to minimize deviation and ensure that all indicator values fell within the range of 0 to 1. Equation (2) shows the formula for Z-score standardization and min–max normalization.

$$Z\text{-}score\colon Z = \frac{Score - Mean}{Standard\ Deviation}$$

$$Min - Max\colon V_i = \frac{X_i - X_{\min}}{X_{\max} - X_{\min}} \tag{2}$$

2.2 Method of vulnerability diagnosis

2.2.1 Vulnerability to heat wave and flood

South Korea's National Climate Change Adaptation Center provides a web platform called the Vulnerability Assessment Tool to Build a Climate Change Adaptation Plan (VESTAP: https://vestap.kei.re.kr) that offers various data sources on climate change scenarios that have been scientifically analyzed. In this study, the RCP 8.5 scenario data for heat waves and heavy rainfall for the years 2030, 2040, and 2050 provided by VESTAP were utilized to describe climate exposure spatially (Table 1).[24] The underlying data for the RCP 8.5 scenario used to describe heat waves include the number of days with a maximum temperature of 30 °C or higher for April–October, the sum of insolation for April–October using logarithmic values, the number of days with a heat index of 32 or higher, the heat wave duration index (HWDI), the number of

Table 1
Parameters for multivulnerability diagnosis.

S. No.	Category	Input data	Spatial unit	Reference
1.	Climate impact	**Extreme heat** Number of days during April–October with maximum temperature >30 °C; number of days during April–October with maximum temperature >35 °C; sum of insolation from April–October in log values; number of days with heat index ≥32; HWDI; felt temperature	Minimum administrative boundary	VESTAP https://vestap.kei.re.kr
		Extreme precipitation Maximum precipitation per day; 5-day cumulative precipitation (mm); annual precipitation (mm); number of days with precipitation ≥80 mm/day; number of days with precipitation ≥150 mm/day		
2.	Population	Total, productive, infant, primary school, and elderly populations	100 m² mesh (total 38523 cells)	National Spatial Information Portal http://www.nsdi.go.kr http://map.ngii.go.kr
3.	Buildings	Coverage ratio, FAR, main structure, residential area, main applications, ground floors, underground floors, year of approval		
4.	Accessibility to community facilities	General hospital, emergency hospital, public health center, day care center, kindergarten, elementary school, park	500 m² mesh	
5.	Economical aspects	Published land prices, individual house prices	100 m² mesh (total 38523 cells)	
6.	Geographical aspect	Altitude difference from sea level		

days with a maximum temperature of 35 °C or higher, and the felt temperature. To account for heavy rainfall as a cause of flooding, the RCP 8.5 scenario data were calculated using maximum daily precipitation, 5-day cumulative precipitation, annual precipitation, number of days with 80 mm/day precipitation, and number of days with 150 mm/day precipitation. The average of the indicator values for heavy rainfall was used as the exposure index for flooding. To minimize the numerical deviation caused by the different base units used in the underlying data obtained from various fields related to weather, cities, and architecture, a common *Z*-score standardization and min–max normalization process were applied to the scenario values describing heat waves and heavy rainfall used as input data (Fig.1).

2.2.2 Sensitivity to heat wave and flood

In this study, the sensitivity of the urban areas to climate change was limited to three categories: population, buildings, and accessibility to major facilities (Table 1). These categories were selected on the basis of their availability in publicly available geographical information. Population data included the total population and specific age groups such as infants, elementary school students, and the elderly. Building data included floor area ratio, floor space ratio, number of floors above and below the ground, residential area, and years of use. Public facility data included daycare centers, kindergartens, elementary schools, general hospitals, emergency facilities, hospitals, health centers, and neighborhood parks. To quantify the sensitivity of these
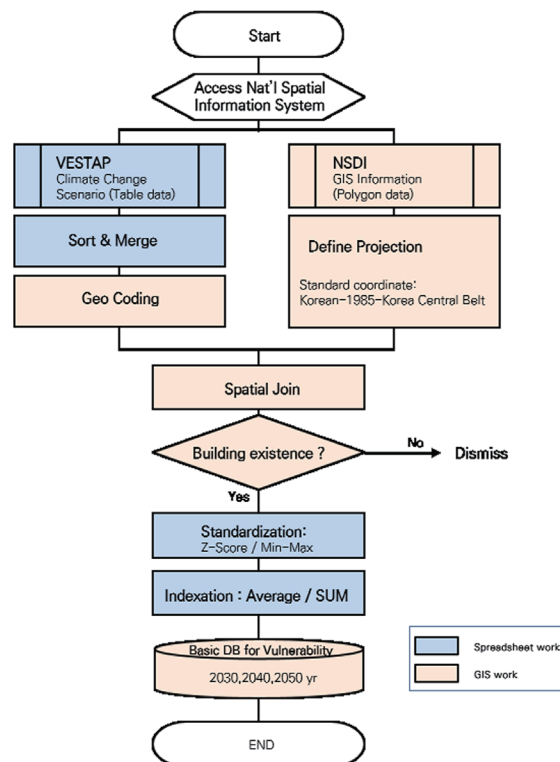

Fig. 1.   (Color online) Flow chart of setting up basic database for vulnerability diagnosis.

components, we used the access distance, which is the distance traveled by road to a public facility.

Buildings were further categorized into two groups on the basis of their vulnerability to different climate hazards: those more susceptible to damage from heat waves owing to high floor area ratio, floor space ratio, and number of floors above ground, and those more susceptible to flooding owing to high floor area ratio and number of floors below ground. Residential areas and years of use were considered common factors affecting the sensitivity to both heat waves and floods.

2.2.3 Adaptive capacity

Adaptive capacity is defined as a combination of geographic and economic characteristics that enable communities to respond to or overcome the impacts of climate change. To measure economic characteristics, we used land values and individual house prices (Table 1). Land value refers to the value of the land, while house prices account for the value of buildings. Both can be used as indicators to evaluate the economic value of prevention or post-disaster response. In terms of geographic characteristics, we divided the terrain into low and high areas on the basis of their elevation above sea level and used the difference in elevation as the basis for measuring adaptive capacity.

2.3 Study area

This study focuses on a central region in South Korea (36.6431–36.3504°N, 127.2892–127.5018°E) that has undergone rapid urbanization. Sejong City was designated the national administrative capital in 2012, and Cheongju City was promoted to an integrated city in 2014, bringing together three cities with a population of more than 300000 in one area, along with the existing Daejeon Metropolitan City (Fig. 2). The total population of this united urban area is about 2.65 million as of 2019, making it the largest population center on the same latitude in South Korea. Given the recent rapid growth of Sejong City and its attraction to the surrounding population, it is important to examine its vulnerability to future climate change in this expanded urban area.

2.4 Designing a combined heat and flood vulnerability diagnostic model

2.4.1 Design of basic frame

We categorized indicators related to heat waves and heavy rainfall into six types of spatial information for the cities studied, considering the increase and decrease in the frequency of these events under the RCP 8.5 scenario in 2030, 2040, and 2050 (Table 1). On the basis of the spatial vulnerability diagnosis results, four categories were developed: HH, high vulnerability to both heat waves and heavy rain; HL, high vulnerability to heat waves only; LH, high vulnerability to flooding due to heavy rain only; and LL, low vulnerability to both heat waves

Fig. 2.   (Color online) Research area: the metropolitan area in the middle of S. Korea (Daejeon city, Sejong city, Cheongju city). Total population: 2656345 (Daejeon: 1484398, Sejong: 319066, Cheongju: 852881) and total area: 1945.23 km^2 (Daejeon: 539.53 km^2, Sejong: 464.9 km^2, Cheongju: 940.8 km^2).[25]

and heavy rain. The minimum spatial unit used was a square with an area of 1 ha (100 m width and 100 m length). The results of the inundation vulnerability diagnosis for heat waves and heavy rainfall were obtained for each year between 2030 and 2050 and displayed on a grid with the minimum spatial resolution. A space was classified as highly vulnerable if it was found to be highly vulnerable at least once per year.

2.4.2 Logical structure of multidiagnosis for climate vulnerability

Urban areas are expected to face increased frequencies of both heat waves and heavy rainfall owing to climate change, resulting in different causes and damage processes. To address this issue, a model that can simultaneously determine the heat and flood vulnerabilities of a unit space in a city is required.[26] Although these events have different pathways from occurrence to damage, the environmental conditions and architectural characteristics of a city can act as common variables that determine the extent of the damage caused by both heat waves and floods. Therefore, we developed a logical structure to process each space affected by the heat wave and flooding processes as a separate variable, utilizing the environmental and building characteristic variables that describe each region in the 2030, 2040, and 2050 climate change scenarios (RCP 8.5) as the basic spatial unit. The heat wave and inundation diagnosis results were statistically clustered into 95% normal distributions, and bivariate Moran's *I* of the Local Indicators of Spatial Association (LISA) analysis was used to complete the logistic system that combined urban heat wave and inundation vulnerabilities.

2.4.3 Vulnerability diagnosis function with spatial variables based on disaster characteristics

The cause of urban heat waves is solar radiation, whereas that of urban flooding is the backflow from overwhelmed drainage systems after heavy rainfall. Both types of hazard affect urban structures and people. Vulnerability to urban heat waves is determined by prolonged exposure to solar radiation, whereas vulnerability to urban flooding is determined by direct exposure to rainwater.[27] Considering these disaster characteristics, diagnostic functional expressions were developed to describe each vulnerability. Vulnerability diagnosis is a process of diagnosing vulnerability based on publicly available statistical data.

The indicators used as exposure variables in the vulnerability diagnostics describe the occurrence characteristics of heat waves and floods for 2030, 2040, and 2050 under the RCP 8.5 scenario. These indicators are applied for the basic administrative region as the minimum spatial extent for both urban heat waves and flooding. All variables were calculated as the average of the individual indicator values per sector to ensure that the impact of the exposure variables was uniform across sectors.

The vulnerability function for urban heat waves consists of a sensitivity variable and an adaptive capacity variable that take into account the height of buildings and the shielding provided by the shadows cast by physical structures. For the population variable, the total population that could be affected and the population density of infants, elementary school students, and the elderly were considered. Since buildings with larger areas exposed to solar radiation are more vulnerable to heat waves, variables such as coverage ratio (horizontal area), floor area ratio (vertical area), residential area, number of floors (height), and building age were used to increase the sensitivity. Indicators related to outdoor activities in urban environments were also included. Walking distances to hospitals, educational facilities, and parks were considered to be sensitizing variables. Adaptive capacity variables, such as economic capacity and topography, were also included to determine vulnerability. Economic capacity was calculated using variables such as the population density of the productive population, and housing and land prices in a region. These indicators have been combined as

$$
\begin{aligned}
V_{heat} = E_{HY} + \Bigg\{ & \left(\frac{P_{all} + P_h + P_e + P_o}{4} \right) \\
& + \left(\frac{B_{CR} + B_{FAR} + B_{RA} + B_{FA} + B_{Age}}{5} \right) + \left(\frac{H_{GH} + H_{EM} + H_H + H_{PH}}{4} \right) \\
& + \left(\frac{E_{DC} + E_K + E_E + P_{park}}{4} \right) \Bigg\} - \Bigg\{ \left(\frac{P_p + B_{UF} + L_{gap} + C_H + C_L}{5} \right) \Bigg\},
\end{aligned}
\tag{3}
$$

where V_{heat} is the heat vulnerability, E_{HY} the heat exposure index of a future year, P_{all} the total population index, P_p the productive population, P_e the elementary school population index, P_o the elderly population index, B_{CR} the coverage ratio index, B_{FAR} the FAR index, B_{RA} the

residential area index, B_{UF} the underground floor index, B_{Age} the building age index, H_{GH} the general hospital accessibility index, H_H the hospital accessibility index, H_{EM} the emergency medical facilities accessibility index, H_{PH} the public health center accessibility index, E_{DC} the daycare accessibility index, E_K the kindergarten accessibility index, E_E the elementary school accessibility index, P_{park} the neighborhood park accessibility index, L_{gap} the average altitude gap index, C_H the individual house price index, and C_L the published land price index [Eq. (3)].

The sensitivity and adaptive capacity variables in the urban flooding vulnerability function were selected on the basis of the characteristics of urban flooding. The population-related indicators for the sensitivity variable of urban flooding were the same as those for heat waves: total population and population densities of infants, elementary school students, and the elderly. Wider buildings with more underground floors are more vulnerable to damage in the case of flooding. In addition, as the drainage system is affected by aging, we applied the relevant floor area ratio, residential area, groundwater level, and age of the building as sensitivity variables. Outdoor urban facilities such as hospitals, educational facilities, and parks are more susceptible to heavy rainfall; therefore, the travel distance from each facility was applied as a sensitivity variable. Adaptive capacity variables are related to the ability to recover from damage and include economic capacity represented by the number of economically active people, land prices, and housing prices. Equation (4) was set as an adaptive capacity variable because the higher the floor area ratio and height of the building, the less damage per unit area, and the faster the building can be restored to normal conditions.

$$V_{flood} = E_{FY} + \left\{ \left(\frac{P_{all} + P_h + P_e + P_o}{4} \right) \right.$$
$$+ \left(\frac{B_{CR} + B_{RA} + B_{UF} + B_{Age}}{5} \right) + \left(\frac{H_{GH} + H_{EM} + H_H + H_{PH}}{4} \right)$$
$$\left. + \left(\frac{E_{DC} + E_K + E_E + P_{park}}{4} \right) \right\} - \left(\frac{P_p + B_{UF} + B_{FAR} + L_{gap} + C_H + C_L}{6} \right) \tag{4}$$

Here, V_{flood} is the flood vulnerability, E_{FY} the flood exposure index of the future year, P_{all} the total population index, P_b the infant population index, P_p the productive population, P_e the elementary school population index, P_o the elderly population index, B_{CR} the coverage ratio index, B_{FAR} the FAR index, B_{RA} the residential area index, B_F the floor index, B_{UF} the underground floor index, B_{Age} the building age index, H_{GH} the general hospital accessibility index, H_H the hospital accessibility index, H_{EM} the emergency medical facilities accessibility index, H_{PH} the public health center accessibility index, E_{DC} the daycare accessibility index, E_K the kindergarten accessibility index, E_E the elementary school accessibility index, P_{park} the neighborhood park accessibility index, L_{gap} the average altitude gap index, C_H the individual house price index, and C_L the published land price index [Eq. (4)].

3. Results and Discussion

3.1 Geospatialization of input variables

The South Korean government has provided information on projected heat waves and heavy rainfall for the RCP 8.5 scenario in 2030, 2040, and 2050 at the administrative division level. To capture the wide spatial scope of climate change impacts, the exposure variables for heat waves and heavy rainfall were scaled down to the smallest administrative division in South Korea. The heat wave exposure variable was color-coded such that dark red indicates a high exposure level, whereas the heavy rainfall exposure variable was color-coded such that dark blue indicates a high exposure level (Fig. 3).

The study area was divided into 1 ha grids to maximize the spatial resolution, resulting in 196561 grids of 100×100 m^2. Among them, 38523 grids contained the populations and buildings studied. All information used in the sensitivity and adaptive capacity variables was spatially represented on a 1 ha grid. Combining the three RCP 8.5 scenarios, the two exposure variables (heat wave and heavy rain), sensitivity and adaptive capacity variables, and the 22 spatial parameters were used in the vulnerability diagnosis calculation.
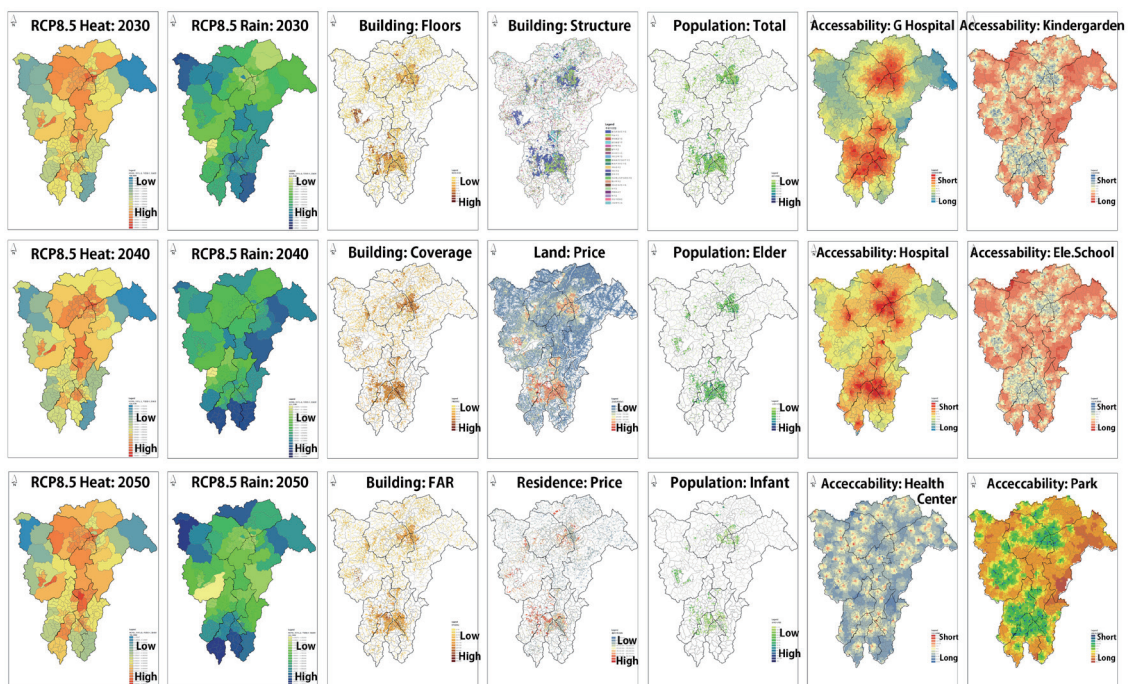

Fig. 3. (Color online) Results of spatialization of input information.

3.2 Spatial diagnostics of heat wave and flooding vulnerability

The logic model shown in Fig. 4 was used to determine the vulnerability to urban heat waves and floods at a spatial unit of 1 ha, wherever buildings existed in the study area. To obtain vulnerability at the spatial level, all sensitivity and adaptive capacity variables, except the exposure variables, were included in the standardized and normalized equation [Eq. (2)], along with the corresponding raw statistical information at a 1 ha spatial unit (Fig. 3). Using GIS, the exposure, sensitivity, and adaptive capacity information were input for the same locations by computing the heat wave vulnerability functions [Eq. (3)] and flood vulnerability functions [Eq. (4)]. Thus, the buildings and inhabited locations in 2018 were found to be vulnerable to heat waves and flooding when exposed to heat waves and heavy rainfall events in 2030, 2040, and 2050 under the RCP 8.5 scenario.
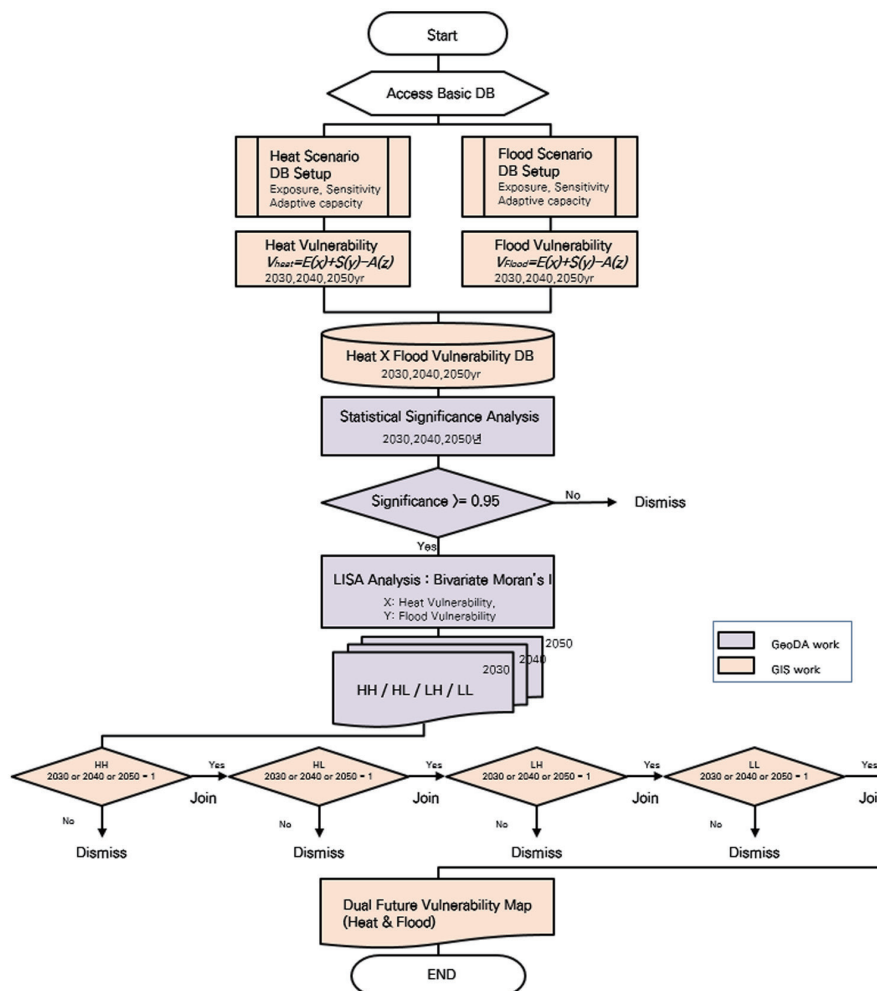

Fig. 4.   (Color online) Flow chart of making the dual future vulnerability map.

The analysis process was designed to express the diagnostic results as follows: HH, high vulnerability to both heat waves and urban flooding; HL, high vulnerability to heat waves only; LH, high vulnerability to urban flooding only; and LL, low vulnerability to both. Bivariate Moran's *I* in the LISA model was applied to diagnose multiple climate disaster vulnerabilities on the basis of these quadrants, using heat vulnerability on the x-axis and urban flood vulnerability on the *y*-axis. The LISA model used the default program GeoDA 10.2, where the first quadrant represents a high vulnerability to both heat waves and urban flooding, whereas the second quadrant represents a high vulnerability to urban flooding. The third quadrant represents low vulnerability to both heat waves and flooding, and the fourth quadrant represents high vulnerability to heat waves only. Moran's *I* distribution showed clustering characteristics for both heat waves and urban flood vulnerabilities, indicating a tendency towards high randomness and low autocorrelation (Fig. 5).

In summary, in this study, we assessed the vulnerability of buildings and inhabited spaces in South Korea to the combined impacts of heat waves and urban flooding under different RCP 8.5 scenarios for 2030, 2040, and 2050. We utilized a 1 ha spatial resolution grid to maximize the spatial resolution of the analysis. The vulnerability assessment was based on multiple variables related to exposure, sensitivity, and adaptive capacity. The analysis was carried out using the LISA model to diagnose multiple climate disaster vulnerabilities in accordance with the four quadrants of a quadratic function graph. The results showed the spatial distribution of heat wave and urban flooding vulnerabilities in terms of the type of unit space with inhabited buildings. The findings of this study can be useful for urban planning and designing projects to improve the resilience of the current environment based on climate change vulnerability.

3.3   Analyzing the characteristics of vulnerable areas for urban planning

It is important to have information linking vulnerability to spatial characteristics in order to establish urban planning that is resilient to natural disasters caused by climate change. By identifying the characteristics of cities based on vulnerability type, we can establish a foundation
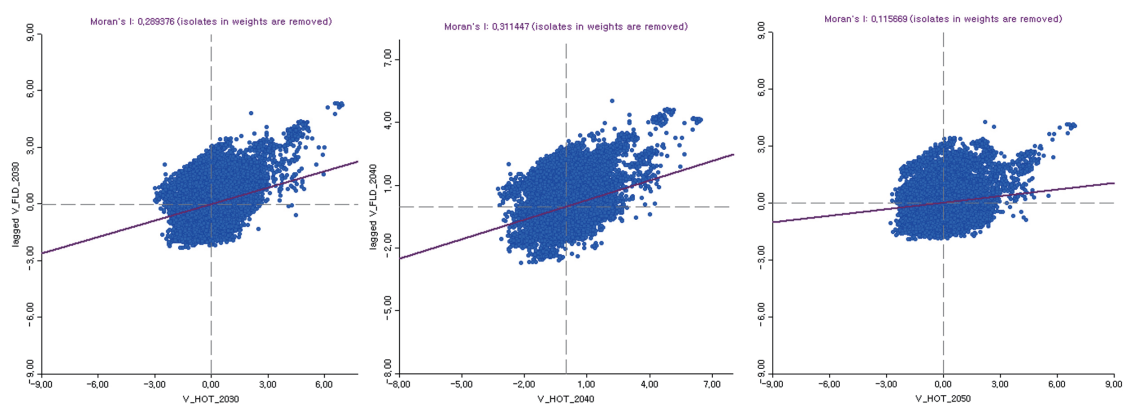

Fig. 5.   (Color online) Cluster characteristics and trend functions using bivariate Moran's *I* (2030, 2040, 2050 in order).

for reconstructing the physical spatial structure of mid- to long-term urban planning. Out of a total of 38523 one-hectare unit spaces, we have selected and analyzed 25467 units with a statistically significant 95% confidence interval, on the basis of the physical characteristics of cities by vulnerability type (Fig. 6). The descriptive statistical values presented in this analysis are the actual means before the standardization of the population by type of a 1 ha unit space, except for exposure. These findings will be informative to urban planners designing strategies to improve the resilience of cities to future climate change (Table 2).

The four types of vulnerability to heat waves and flooding (HH, HL, LH, and LL) were established on the basis of their respective levels of vulnerability. Climate exposure values were obtained from the underlying data describing exposure to heat waves and heavy rainfall under the RCP 8.5 scenario and then normalized to a maximum value of 1 and a minimum value of 0 based on the intensity of exposure. Type HH had an exposure value of approximately 0.5 for both heat waves and heavy rainfall. Type HL was found to have significantly higher exposure to heat waves of approximately 0.7 and the heavy rainfall index of approximately 0.3. Type LH was identified as having higher exposure to heavy rainfall, with a heat index below 0.3 and a heavy rain index above 0.6. Type LL was found to have high exposure to heat waves, with a difference in exposure values of 0.5 or more for heat waves and 0.4 for heavy rainfall when compared with all other types. This can be interpreted as a set of regions with high environmental exposure but low vulnerability owing to the physical environment.

Housing and land prices in the study area vary depending on the type of vulnerability (Table 3). The LL area had the highest housing price, with an average of Korean Won (KRW)
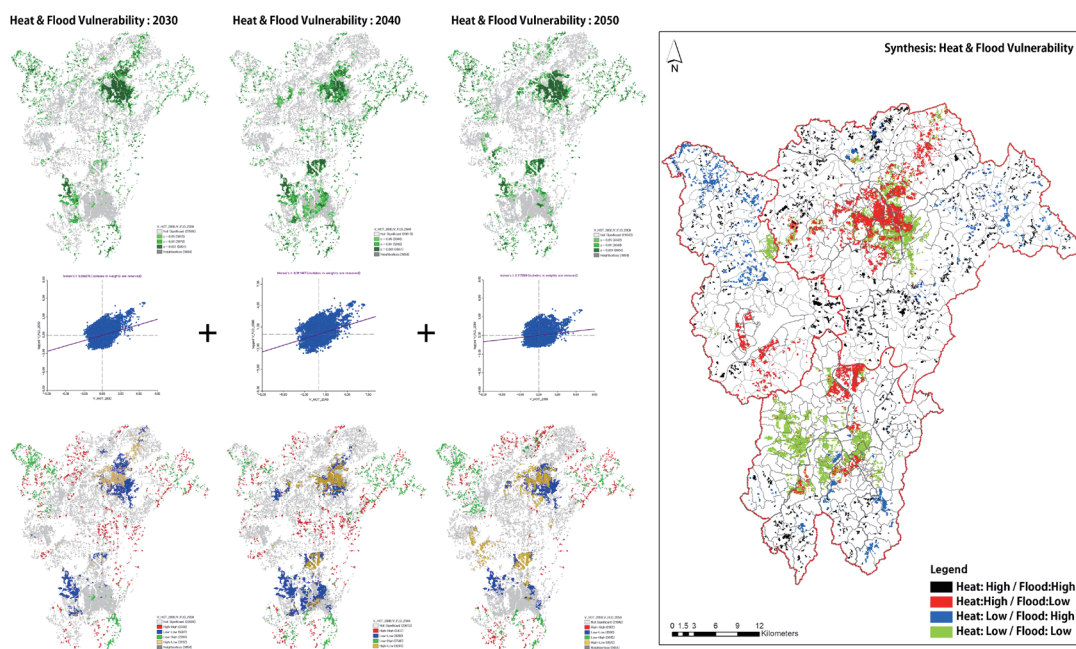

Fig. 6.   (Color online) Typology maps of urban heat wave–flooding vulnerability assessments for years 2030, 2040, and 2050.

Table 2
(Color Online) Population characteristics (People per Hectare) by vulnerability group (red: more vulnerable, green: less vulnerable).

Type of vulnerability	Total population	Working age population	Infant population	Elementary school-age population	Elderly population
HH	8.2	4.8	0.3	0.2	1.4
HL	123.3	90.2	8.5	8.1	13.6
LH	19.2	13.1	0.7	0.6	3.1
LL	113.4	84.4	6.3	6.4	13.5

Table 3
(Color Online) Trends in individual homes and listings by vulnerability group (red indicates high values).

Type of vulnerability	Individual housing area (thousand won)	Announced land price (KRW 1000/m^2)
HH	57710	83
HL	86070	376
LH	71850	140
LL	105710	540

105710000, whereas the HH area had the lowest housing price, with an average of KRW 57710000. In terms of land prices, the LL area had the highest value at 540000 won/m^2, followed by the HL area at 376000 won/m^2, the LH area at 140000 won/m^2, and the HH area at 83000 won/m^2. Thus, areas with high vulnerability tended to have lower housing and land prices. These findings suggest that housing and land prices are influenced by the level of vulnerability to natural disasters caused by climate change.

We analyzed the general characteristics of buildings in the study area in terms of the vulnerability type (Table 4). Buildings in HH areas, which have a high combined vulnerability to heat waves and floods, were found to be old, low rise, and small. The average completion year was 1987, with a building-to-land ratio of 18.8%, floor area ratio of 23.0%, and average house area of 82.3 m^2. HL-area buildings were completed, on average, in 1998, used for 20.3 y, and had a building-to-land ratio of 32.0%, a floor area ratio of 75.0%, and an average house area of 100.8 m^2. LL-area buildings were completed, on average, in 1999, used for 18.8 years, and had a building-to-land ratio of 29.2%, floor area ratio of 74.9%, and average house area of 103.5 m^2, the largest among all types. The physical features of the HL and LL areas were similar. The LH area included medium-sized buildings that were completed in 1991, used for 26.6 y, and had a building-to-land ratio of 21.1%, a floor area ratio of 29.6%, an average of 1.4 stories, and an average residential area of 90.9 m^2.

Buildings in the study area were classified by vulnerability type and analyzed in terms of their structures and main uses (Table 5). Brick structures were the most common in HH areas; other types of structure include lightweight steel frames, general wooden structures, general steel frames, reinforced concrete structures, and block structures. Reinforced concrete structures accounted for over 40% of buildings in HL areas, followed by brick structures at over 20%, whereas general steel frames and lightweight steel frames each accounted for approximately 10%. The LH area had characteristics similar to those of the HH area, with brick structures being the most common, followed by lightweight steel frames, general wooden structures,

Table 4
(Color Online) Building characteristics by vulnerability group (red indicates high values).

Type of Vulnerability	Building-to-land ratio (%)	Floor area ratio (%)	Residential area (m^2)	Number of ground floors (floor)	Number of basement floors (floor)	Period of use (y)
HH	18.8	23.0	82.3	1.3	0.1	31.0
HL	32.0	75.0	100.8	4.2	0.5	20.3
LH	21.1	29.6	90.9	1.4	0.2	26.6
LL	29.2	74.9	103.5	4.2	0.7	18.8

Table 5
(Color Online) Main structures of buildings by vulnerability group (red indicates high values).

Type of structures	HH	HL	LH	LL
Other structure	4	1	5	2
Container tank	1	0	2	0
Prefabricated panel	1	0	1	0
Log structure	3	1	1	2
General wood structure	905	217	508	153
Wooden structure	2	0	0	0
Steel-reinforced concrete structure	2	12	10	32
Steel-framed concrete structure	10	7	3	12
Other steel structure	4	3	9	5
Steel pipe structure	179	47	136	32
Lightweight steel structure	964	608	738	788
General steel structure	625	980	455	944
Other concrete structures	0	2	0	1
Precast concrete structure	1	5	0	10
Reinforced concrete structure	596	3137	643	4607
Other masonry structures	66	43	29	17
Steel House Joe	0	0	0	0
Stone structure	2	1	0	0
Block structure	279	134	220	160
Brick structure	1844	1935	1229	2051
Masonry structure	3	5	2	3

reinforced concrete, general steel frames, and block structures. The LL area showed a pattern similar to that of the HL area, but with reinforced concrete structures accounting for over 50% and brick structures for more than 20% of the buildings. In the HL and LL areas, buildings were recently built, and the sum of reinforced concrete and brick structures accounted for over 50%. In HH and LH areas, more than 50% of buildings had relatively weak structural strength, including brick, wooden, and lightweight steel structures.

Most buildings in the study area were detached houses, but the HH and LH areas had nearly 70% multiunit housing (Table 6). The HL and LL areas had a high percentage of Class 1 and 2 Neighborhood Living Facilities related to commercial facilities. In the HH and LH areas, the use of convenience facilities was relatively low, whereas the ratios of detached houses, animal- and plant-related facilities, factories, and warehouses were relatively high. This suggests that the environment in detached housing areas is related to livelihood. In HL and LL areas, the ratio of

Table 6
(Color Online) Primary uses of buildings by vulnerability group (red indicates high values).

Type of facility	HH	HL	LH	LL
Tourist rest facility	6	1	0	6
Cemetery-related facilities	0	0	0	0
Broadcasting communication facility	1	1	0	6
Corrections and military facilities	0	0	0	2
Manure and waste disposal facilities	14	14	7	8
Animal- and plant-related facilities	342	78	226	63
Automobile-related facilities	12	58	16	113
Dangerous goods storage and disposal facilities	18	45	33	75
Warehouse facility	221	140	173	160
Factory	320	521	222	372
Accommodation	12	22	3	46
Business facilities	3	26	4	69
Exercise facility	1	9	3	28
Training facility	0	0	3	1
Facilities for the elderly	52	32	35	51
Education research facility	16	97	21	310
Medical facility	1	6	2	19
Transportation facility	0	2	2	3
Sales facility	3	12	0	32
Religious facilities	13	15	11	56
Cultural and assembly facilities	5	9	5	18
Class 2 Neighborhood Living Facility	376	841	330	1124
Class 1 Neighborhood Living Facility	180	506	159	632
Apartment house	36	1302	60	1666
House	3859	3401	2676	3959

detached houses was 50%, the ratio of apartments was close to 20%, and the ratio of neighborhood living facilities was high; therefore, it can be expected to be a positive environment in terms of living convenience.

We also analyzed the accessibility and distance of hospitals, educational facilities, and parks in terms of vulnerability type (Table 7). LL areas, with low vulnerability to heat waves and floods, showed high accessibility to hospitals, with an average distance of 3.64 km for general hospitals, 2.94 km for emergency medical facilities, 2.54 km for hospitals, and 2.6 km for public health centers. Educational facilities and parks were accessible within 1 km. In contrast, high-vulnerability areas had reduced access to health facilities, especially HH and LH areas with high composite and flood vulnerabilities. In these areas, medical facilities were more than 10 km away. Educational facilities and parks were also located at an average distance of approximately 5 km. The HL area, which is highly vulnerable to heat waves, had a reasonable distance of 4–5 km to medical facilities; however, educational facilities and parks were within easy walking distances. These findings reveal the characteristics of insufficient urban planning facilities in terms of vulnerability types and highlight the importance of considering accessibility to critical facilities in urban planning for adaptation to climate changes.

Table 7
(Color Online) Distance (km) to healthcare, education, parks, and green spaces in different vulnerability groups (red: high vulnerability, green: low vulnerability).

Type of vulnerability	General hospital	Emergency medical care center	Hospital	Public health center	Day care center	Kindergarten	Elementary school	Life zone park
HH	14.27	12.14	10.44	3.93	5.27	4.68	4.77	6.10
HL	5.06	4.79	4.11	2.85	0.96	1.19	1.35	1.54
LH	15.12	11.52	10.86	2.91	3.15	3.08	2.99	4.53
LL	3.64	2.94	2.54	2.60	0.60	0.86	1.00	0.89

4. Conclusions

The objective of this study was to establish a methodology for identifying vulnerability based on the current state of a city, in anticipation of complex natural disasters resulting from climate change. By analyzing the spatial characteristics that contribute to vulnerability, it is possible to propose urban structures and design alternatives for buildings that can enable effective response to future climate scenarios. To minimize the impact of natural disasters on the lives of residents, a complex vulnerability analysis model was developed on the basis of the current state of facilities and utilization of public space. We analyzed the vulnerability of target cities to heat waves and urban floods, which are causing threats to life and property in Korea with increasing frequency. The model uses the climate change vulnerability function set by the IPCC and indicators necessary for urban design to derive a flexible function in the form of Eqs. (3) and (4). The sensitivity index is based on the affected population and building-related information. Adaptive capacity is measured by accessibility to hospitals and parks. Our approach aligns with the climate change policy established by the international community and can be adjusted to local situations and objects. Using this model, our aim was to develop urban structures and design alternatives for buildings that can respond to future climate scenarios.

In this study, the cities of Daejeon, Sejong, and Cheongju were analyzed as a single zone to diagnose the climate vulnerability of building clusters within each zone. The vulnerable points were compared in terms of their spatial distributions and regional characteristics. The results showed that building cluster areas could be divided into those vulnerable to both heat waves and floods, those with high heat wave vulnerability, those with high flood vulnerability, and those with low vulnerability to both heat waves and floods. The vulnerability analysis used sensitivity and adaptability indicators to identify the detailed characteristics of the buildings and facilities that make up the city. It was found that areas vulnerable to both heat waves and floods have a small number of residents and a high ratio of aged, detached houses made of brick that have low economic feasibility as real estate. Accessibility to major facilities, such as hospitals, parks, and schools, is also poor. Therefore, urban designs that include areas vulnerable to both heat waves and floods should focus on improving the performance of old and detached houses and enhancing the accessibility of residents of these houses to major facilities.

It is crucial to recognize that a city's sociological function is interconnected with its resilience, and improving social capacity can have a more significant impact on resilience than enhancing physical function. Although vulnerability is used to measure resilience, the precision of sociological indicators such as population and land value is limited. Therefore, identifying and applying indicators of a city's social capacity are crucial future research tasks to accurately diagnose vulnerabilities. If the results of the vulnerability diagnosis are collected periodically, they can serve as a tool to monitor the improvement of vulnerable areas and increases in vulnerability. If various climate-change-induced natural disaster impact factors are applied to climate exposure variables other than heat waves and floods, it will be possible to identify current vulnerabilities in accordance with future scenarios and to use them as a basis for preparedness. The process of utilizing future climate change scenarios for natural disaster vulnerability assessment should be further studied for application in policies dealing with preventive safety, including urban and building policies. The use of vulnerability assessments as a basis for creating criteria for a location and spatial design of new development areas and zoning to improve the vulnerability of older urban centers should be the foundation for creating sustainable cities and buildings in the future. In a follow-up study, it would be valuable to develop a rationale for the designation of districts related to natural disaster prevention as well as for the regulation of development activities in those districts.

In this study, we enhanced climate vulnerability diagnosis and urban planning using sensors. We identified microlocations vulnerable to heat waves and flooding, focusing on buildings. This contributed to optimal sensor placement, reduced building and regional vulnerabilities, and efficient continuous monitoring points.

(1) Comprehensive Compound Natural Hazards Approach: Unlike previous studies, this research focuses on the simultaneous vulnerability assessment of buildings to heat waves and urban flooding. Examining compound hazards centered on buildings enables the identification of potential risks in areas with high concentrations of vulnerable buildings, providing insights for effective urban planning.

(2) Spatial Vulnerability Analysis: Emphasizing the importance of spatial factors, specific characteristics contributing to vulnerability are analyzed. By considering architecture and demographics, vulnerable areas are identified and urban responses to address future climate scenarios effectively are proposed.

(3) Optimal Sensor Placement for Vulnerability Mitigation: Utilizing vulnerable area locations and building characteristics identified in the study, optimal sensor installation sites can be determined. These sensors can forecast heat waves and flooding, triggering alarm systems and guiding the placement of continuous weather monitoring facilities centered on vulnerable buildings.

(4) Local Climate Adaptation and Policy Relevance: Aligned with international climate change policies, we also consider local context and goals. The proposed methodology can be adapted and applied to specific situations, offering practical value in urban planning and policy decision-making processes.

By highlighting these aspects, the results of this study provide distinctiveness and original concepts to the field of climate vulnerability assessment and urban planning. The findings

contribute to formulating strategies and interventions for sensor utilization, enhancing city resilience, and mitigating the impacts of climate-change-induced natural hazards.

Acknowledgments

References

1   Weather data open portal: https://data.kma.go.kr/climate/heatWave (accessed 31 May 2019).
2   Thermal disease monitoring system of the Integrated Health and Disease Management System by the Korea Centers for Disease Control and Prevention: https://kdca.go.kr/ (accessed 31 May 2023).
3   Korea Meteorological Administration: Top 10 Torrential Rains: Lessons Learned from the Last 20 Years (Korea Meteorological Administration, Seoul, 2012) 1st ed., pp. 6–9.
4   International Institute for Sustainable Development: https://www.iisd.org/project/advancing-alignment-climate-resilient-development (accessed 31 May 2019).
5   United Nations Office for Disaster Risk Reduction: https://www.undrr.org/ (accessed 31 May 2019).
6   United Nations, Asian Development Bank, and United Nations Development Programme: Transformation towards Sustainable and Resilient Societies in Asia and the Pacific (2018).
7   United Nations Climate Change Secretariat: Technical paper by the secretariat (2017).
8   A. Sharifi and Y. Yamagata: Energy Procedia. **61** (2014) 1491. https://doi.org/10.1016/j.egypro.2014.12.154
9   NYC Mayor's office of Recovery and Resiliency: Climate Resiliency Design Guidelines, ver.3.0, NYC (2019).
10 S. C. Holling: Annu. Rev. Ecol. Systematics **4** (1973) 1.
11 R. J. T. Klein, R. J. Nicholls, and F. Thomalla: Global Environ. Change Part B: Environ. Hazards **5** (2003) 35. https://doi.org/10.1016/j.hazards.2004.02.001
12 G. Lance and H. C. Stanley: Panarchy: Understanding Transformations in Systems of Humans and Nature (Washington, DC Island Press, 2002). http://hdl.handle.net/10919/65531
13 S. Meerow and J. P. Newell: Landscap. Urban Plan. **159** (2017) 62. https://doi.org/10.1016/j.landurbplan.2016.10.005
14 R. Leichenko: Curr. Opin. Environ. Sustain. **3** (2011) 164. https://doi.org/10.1016/j.cosust.2010.12.014
15 Y. Jabareen: Cities **31** (2013) 220. https://doi.org/10.1016/j.cities.2012.05.004
16 D. Serre, B. Barroca, M. Balsells, and V. Becue: J. Flood Risk Manag. **11** (2016) 69. https://doi.org/10.1111/jfr3.12253
17 A. Feliciotti, O. Romice, and S. Porta: Open House Int. **41** (2016) 23. https://doi.org/10.1108/OHI-04-2016-B0004
18 P. Benjamin, E. Yuen, and R. Westaway: Sustain. Sci. **6** (2011) 177. https://doi.org/10.1007/s11625-011-0129-1
19 L. Berrang-Ford, A. R. Siders, A. Lesnikowski, A. P. Fischer, M. W. Callaghan, N. R. Haddaway, K. J. Mach, M. Araos, M. A. R. Shah, M. Wannewitz, D. Doshi, T. Leiter, C. Matavel, J. I. Musah-Surugu, G. Wong-Parodi, P. Antwi-Agyei, I. Ajibade, N. Chauhan, W. Kakenmaster, C. Grady, V. I. Chalastani, K. Jagannathan, E. K. Galappaththi, A. Sitati, G. Scarpa, E. Totin, K. Davis, N. C. Hamilton, C. J. Kirchhoff, P. Kumar, B. Pentz, N. P. Simpson, E. Theokritoff, D. Deryng, D. Reckien, C. Zavaleta-Cortijo, N. Ulibarri, A. C. Segnon, V. Khavhagali, Y. Shang, L. Zvobgo, Z. Zommers, J. Xu, P. A. Williams, I. V. Canosa, N. van Maanen, B. van Bavel, M. van Aalst, L. L. Turek-Hankins, H. Trivedi, C. H. Trisos, A. Thomas, S. Thakur, S. Templeman, L. C. Stringer, G. Sotnik, K. D. Sjostrom, C. Singh, M. Z. Siña, R. Shukla, J. Sardans, E. A. Salubi, L. S. S. Chalkasra, R. Ruiz-Díaz, C. Richards, P. Pokharel, J. Petzold, J. Penuelas, J. P. Avila, J. B. P. Murillo, S. Ouni, J. Niemann, M. Nielsen, M. New, P. N. Schwerdtle, G. N. Alverio, C. A. Mullin, J. Mullenite, A. Mosurska, M. D. Morecroft, J. C. Minx, G. Maskell, A. M. Nunbogu, A. K. Magnan, S. Lwasa, M. Lukas-Sithole, T. Lissner, O.Lilford, S. F. Koller, M. Jurjonas, E. T. Joe, L. T. M. Huynh, A. Hill, R. R. Hernandez, G. Hegde, T. Hawxwell, S. Harper, A. Harden, M. Haasnoot, E. A. Gilmore, L. Gichuki, A. Gatt, M. Garschagen, J. D. Ford, A. Forbes, A. D. Farrell, C. A. F. Enquist, S. Elliott, E. Duncan, E. C. de Perez, S. Coggins, T. Chen, D. Campbell, K. E. Browne, K. J. Bowen, R. Biesbroek, I. D. Bhatt, R. B. Kerr, S. L. Barr, E. Baker, S. E. Austin, I. Arotoma-Rojas, C. Anderson, W. Ajaz, T. Agrawal, and T. Z. Abu: Nat. Clim. Chang. **11** (2021) 989. https://doi.org/10.1038/s41558-021-01170-y

20 S. A. Sarkodie and V. Strezov: Sci. Total Environ. **656** (2019) 150. https://doi.org/10.1016/j.scitotenv.2018.11.349.
21 Boston Public Works Department: Climate Resilient Design Standards & Guidelines (For protection of public rights-of-way, City of Boston 2018).
22 F. Taryn, E. Northrop, K. Mogelgaard, and K. Levin: World Resources Institute (2017) 7. http://www.wri.org/publication/NDC-enhancement-by-2020
23 IPCC (2007): Assessing key vulnerabilities and the risk from climate change (Parry, Cambridge University Press, Cambridge, 2007) pp. 7–22.
24 Vulnerability Assessment Tool to build Climate Change Adaptation Plan VESTAP: https://vestap.kei.re.kr (accessed 6 January 2023).
25 EOSDIS Worldview: https://worldview.earthdata.nasa.gov (accessed 13 June 2019).
26 S. Reinhard, A. Kaidel, S. Golz, T. Naumann, J. S. Lopez-Gutierrez, and S. Gravin: ISPRS Int. J. Geo-Inf. **5** (2016) 202. https://doi.org/10.3390/ijgi5110202
27 Garvin Stephen (2017): Flood Resilient Buildings-towards a mainstream activity, BRE (accessed 6 July 2019).

About the Authors

Eunseok Lee received his B.S. degree in environmental and urban engineering from Yonsei University, South Korea, in 2001 and his M.S. and Ph.D. degrees in landscape architecture from the Graduate School of Environmental Studies at Seoul National University, South Korea, in 2007 and 2015, respectively. From 2018 to 2020, he was the head of the National Green Building Center at AURI, South Korea. Since 2015, he has been a research fellow at the Architecture and Urban Research Institute under the Office of the Prime Minister of South Korea. His research interests are in urban studies related to climate change and the assessment of vulnerability using GIS. (enlee@auri.re.kr)